Monitoring cancer treatment: quantitative MRI of tumor micro-structure and metabolism with chemical exchange saturation transfer and diffusion weighted MRI

Rozhin Yousefi[1], Xiaoyong Huang[2], Stanley K. Liu[2], and Greg J. Stanisz[1,2]
[1]*Medical Biophysics, University of Toronto, Toronto, Ontario, Canada,* [2]*Sunnybrook Research Institute, Toronto, Ontario, Canada*

Target Audience: This work will appeal to those interested in the application of quantitative MRI to evaluate tumor response to treatment.

Purpose: Developing an imaging biomarker that provides early assessment of treatment response in cancer patients to significantly enhance treatment outcome. The objective of this study is to assess tumor micro-structure and micro-environment during treatment using quantitative MRI, knowing that changes at the cellular level occur earlier than anatomical changes. To achieve this goal, quantitative MRI measurements were performed using two MRI techniques: chemical exchange saturation transfer (CEST) and diffusion weighted MRI (DW-MRI).

Methods: Mice Xenografts: Animal experiments were performed on SCID mice (n=6). Each mouse was injected intramuscularly with approximately $3x10^6$ DU-145 human prostate cancer cells in a hind leg. The mice tumors were scanned once they reached 0.75 cm in diameter. MRI scanning was performed on a 7 T animal MRI system (Bruker BioSpin). The body temperature of the mice was kept at 37°C during scanning sessions, using a feedback-controlled air heating system. After the first session of imaging, the tumors received a 10 Gy radiation dose using an X-Ray irradiation system (43855 F, FAXITRON BIOPTICS, LLC). Post-treatment MR imaging was performed 72 hours after irradiation.

MRI Acquisition: The images had a field of view of 2.2 × 2.2 cm^2 and a slice thickness of 1mm, with an in-plane resolution of 458 µm. Diffusion-weighted images were acquired over sixteen different effective diffusion times (0.6 ms<TD_{eff} <40 ms) using the Oscillated/Pulsed Gradient Spin Echo sequence (TR/TE=1500/70 ms). For each TD_{eff}, the diffusion gradient strength was varied to obtain images with five different b-values in the range of 0 to 1000 s/mm^2. The applied CEST sequence (TR/TE=501/3.1ms) consisted of a radiofrequency (RF) saturation pulse followed by a spoiled gradient echo. The saturation pulse (amplitude=0.57 µT, duration=490 ms) was applied at an off-resonance frequency range of -2400 to 2400 Hz, at increments of 100 Hz.

Data Analysis: Apparent diffusion coefficient (ADC) values were calculated voxel-wise for each TD_{eff} by knowing that there is a mono-exponential relationship between signal intensity and b-value. [1] For further interpretation of diffusion data, ADCs were fitted to the parallel plane model (PPM) for pre-treatment and post-treatment measurements. [5] This model assumes that diffusion occurs between two permeable infinite parallel planes with the following fitting parameters: d, the distance between the planes; D_{free}, the free diffusion of solvent; and D_{rest}, the restricted diffusion after a long period of time. CEST spectrums were first corrected for B_0 inhomogeneity by shifting the water peak to 0Hz. Signal drift was also corrected using a signal intensity of five reference images acquired at ±200kHz. The resultant CEST spectrum had five distinct peaks, which were modeled by independent Lorentzian shape functions. [2, 3]

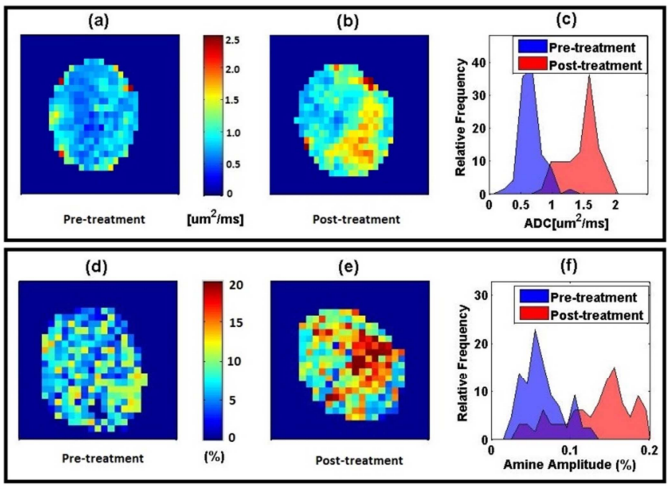

Figure 1: *ADC map and amine CEST map: (a) and (d) pre-treatment, (b) and (e) post-treatment. (c) ADC and (f) amine histogram (# of bins=20).*

Results and Discussion: As an example, pre-treatment and post-treatment ADC maps calculated for one of the sixteen diffusion measurements (OGSE with TD_{eff} =3.75 ms) are shown in Figs. 1 (a) and (b). As can be observed from Fig. 1 (b), there is a region with elevated ADC values in the tumor tissue. In the literature, increased post-treatment ADC has been attributed to response to therapy. [4] To evaluate the ADC changes quantitatively, histograms are plotted in Fig. 1 (c). The summary of PPM-fitted parameters averaged over all seven mice is also presented in Table 1. Decreases in post-treatment "d" are consistent with the cell shrinkage process during apoptosis. CEST peak-fitting showed that CEST peaks differ before and after treatment, most significantly in the amine peak. Amine peak amplitude maps are depicted in Figs. 1 (d) and (e), which demonstrate a significant increase in post-treatment amine amplitude. A similar outcome was observed in all six mice (Table 1).

	ADC [µm²/ms] Mean	Amine Amp [%] Mean	d [µm]	D_{free} [µm²/ms]	D_{rest} [µm²/ms]
Pre-treatment	0.82±0.07	7.59 ± 2.30	5.2±0.4	1.37±0.09	0.56±0.06
Post-treatment	1.28±0.19	11.04 ± 2.01	3.3±0.4	1.72±0.12	1.18±0.07

Table 1: *qMRI parameters averaged over all mice (n=6)*

Conclusion: The changes in ADC and PPM parameters observed in some regions of tumors after 72 hours of irradiation indicate morphological changes, which provide evidence of apoptosis. Metabolic changes were also found in these regions due to a rise in amine CEST amplitude. The origin of this effect, however, is still undetermined. These preliminary results demonstrate the potential of this technique to enhance reliability of MRI assessment of treatment response. Future work is to classify between responders and non-responders by designing an algorithm based on a sufficiently large dataset.

References: 1. Portnoy, S., et al., NMR in Biomedicine 27.4 (2014): 371-380. **2.** Zaiss M., et al., J Magn Reson 2011;211:149-155. **3.** Desmond, K., et al., Magnetic Resonance in Medicine 71.5 (2014): 1841-1853. **4.** Patterson, D., et al., Nature Clinical Practice Oncology 5.4 (2008): 220-233. **5.** Stepisnik J., Phys B 1993;183:343–350.